



Article

# A New Urban Index for Expressing Inner-City Patterns Based on MODIS LST and EVI Regulated DMSP/OLS NTL

Yangxiaoyue Liu <sup>1,2</sup>, Yaping Yang <sup>1,3,\*</sup>, Wenlong Jing <sup>4,5,6</sup> , Ling Yao <sup>1,3</sup> , Xiafang Yue <sup>1,3</sup> and Xiaodan Zhao <sup>1,3</sup>

<sup>1</sup> State Key Laboratory of Resources and Environmental Information System, Institute of Geographic Sciences and Natural Resources Research, Chinese Academy of Sciences, Beijing 100101, China; lyxy@reis.ac.cn (Y.L.); yaoling@reis.ac.cn (L.Y.); lexf@reis.ac.cn (X.Y.); zhaoxd@reis.ac.cn (X.Z.)

<sup>2</sup> University of Chinese Academy of Sciences, Beijing 100049, China

<sup>3</sup> Jiangsu Center for Collaborative Innovation in Geographical Information Resource Development and Application, Nanjing 210023, China

<sup>4</sup> Guangzhou Institute of Geography, Guangzhou 510070, China; jingwl@reis.ac.cn

<sup>5</sup> Key Laboratory of Guangdong for Utilization of Remote Sensing and Geographical Information System, Guangzhou 510070, China

<sup>6</sup> Guangdong Open Laboratory of Geospatial Information Technology and Application, Guangzhou 510070, China

\* Correspondence: yangyp@igsnr.ac.cn; Tel.: +86-137-0133-0604

Received: 25 May 2017; Accepted: 27 July 2017; Published: 29 July 2017

**Abstract:** With the rapid pace of urban expansion, comprehensively understanding urban spatial patterns, built environments, green-spaces distributions, demographic distributions, and economic activities becomes more meaningful. Night Time Lights (NTL) images acquired through the Operational Linescan System of the US Defense Meteorological Satellite Program (DMSP/OLS NTL) have long been utilized to monitor urban areas and their expansion characteristics since this system detects variation in NTL emissions. However, the pixel saturation phenomenon leads to a serious limitation in mapping luminance variations in urban zones with nighttime illumination levels that approach or exceed the pixel saturation limits of OLS sensors. Consequently, we propose an NTL-based city index that utilizes the Moderate-resolution Imaging Spectroradiometer (MODIS) Land Surface Temperature (LST) and Enhanced Vegetation Index (EVI) images to regulate and compensate for desaturation on NTL images acquired from corresponding urban areas. The regulated results achieve good performance in differentiating central business districts (CBDs), airports, and urban green spaces. Consequently, these derived imageries could effectively convey the structural details of urban cores. In addition, compared with the Vegetation Adjusted NTL Urban Index (VANUI), LST-and-EVI-regulated-NTL-city index (LERNCI) reveals superior capability in delineating the spatial structures of selected metropolis areas across the world, especially in the large cities of developing countries. The currently available results indicate that LERNCI corresponds better to city spatial patterns. Moreover, LERNCI displays a remarkably better “goodness-of-fit” correspondence with both the Version 1 Nighttime Visible Infrared Imaging Radiometer Suite Day/Night Band Composite (NPP/VIIRS DNB) data and the WorldPop population-density data compared with the VANUI imageries. Thus, LERNCI can act as a helpful indicator for differentiating and classifying regional economic activities, population aggregations, and energy-consumption and city-expansion patterns. LERNCI can also serve as a valuable auxiliary reference for decision-making processes that concern subjects such as urban planning and easing the central functions of metropolis.

**Keywords:** LERNCI; vegetation coverage; land surface temperature (LST); urban pattern; DMSP/OLS NTL; NPP/VIIRS DNB; WorldPop

## 1. Introduction

As locations where modern industries and populations aggregate, cities are not only one of the key products of human civilization engaged in the process of changing the natural environment, but also the focus of numerous environmental regulation and protection mechanisms. When the natural landscape becomes a largely water-impervious surface because of the impact of human activities, it gradually but significantly influences local vegetation distribution patterns, which then leads to local, and eventually regional, climate changes [1]. As a result, there exist distinct differences between the internal patterns and natural properties of urban and rural areas [2]. With the development of remote sensing techniques, numerous studies have been made to document land-use and land-cover change (LUCC) [3]. However, there is not enough discussion devoted to the spatial patterns of cities around the world [4]. Therefore, there remains a pressing need to have the ability to consistently compare city patterns of both developed and developing countries and within various climate zones.

The Operational Linescan System of the US Defense Meteorological Satellite Program (DMSP/OLS) Night Time Lights (NTL) data consists of NTL images which could be used to express local light intensities and delineate urban patterns. However, NTL images obtained from relatively brightly lit urban locations commonly suffer from pixel saturation because of the limitations of the OLS sensors, which were not specifically designed for imaging urban areas. To overcome the inherent limitations of the OLS sensors, several studies were made to find possible solutions for calibrating and obtaining information from saturated DMSP/OLS NTL data. Letu et al. [5] came up with a cubic-regression equation using non-saturated pixels to rectify the light-intensity values obtained from the saturated pixels, but this method only acted on the administrative region rather than at the pixel level. Letu et al. [6] later developed a pixel-scale model that utilizes non-saturated stable light images from 1999 and radiance calibration images from 1996 to 1997 to effectively increase the variation ranges of saturated pixels. While the correlation between the 1999 NTL data to current ones would continually degrade as time passes and urban patterns change, Ziskin et al. [7] added non-saturated NTL images with low gain settings to images with high gain settings to produce a zero-saturation product. Ziskin's computationally intensive approach is largely inappropriate for individual researchers. Zhuo et al. [8] constructed an Enhanced Vegetation Index (EVI)-based NTL desaturation method to amend pixel-saturated areas based on the anti-atmospheric interference and saturation-resistant characteristics of the EVI. Although this method can be easily implemented, its reliance on only a single parameter (vegetation cover) can limit its effectiveness. The results of these previous attempts at dealing with the pixel-saturation issue seem to point to the need to construct a combined vegetation-and-human-activity-based city index for adequately resolving urban-core patterns.

Many studies have shown that temperature variation signatures of impervious surfaces can substantially differ from those of surfaces covered with vegetation. Chen et al. [9] used temperature variations to analyze the relationship between the urban heat-island effect and land-use changes within the Pearl River Delta Urban Agglomeration. Dousset et al. [10] analyzed the correlation between urban surface temperatures and land cover. Their results showed that in the business and industrial districts, the heat-island effect could result in local temperatures being 7 °C higher than those in other areas. Li et al. [11] demonstrated that the Land Surface Temperature (LST) is a vital parameter in the physics of land-surface processes at local scales.

The aim of this paper is to put forward an LST indicator from the perspective of the urban heat island effect combined with the EVI to build a new, more robust, more widely applicable urban core pattern index. This index is composed of both artificial and natural factors, and it can be used to address the NTL pixel-saturation problem by increasing the effective dynamic range of measurable light intensities.

## 2. Data Resources

### 2.1. Night Time Lights (NTL) Data

The United States DMSP launched polar-orbiting satellites into sun-synchronous orbits of about 830 km altitude [12]. These satellites go on daily 12-h observation periods for obtaining global cloud

distribution and cloud-top temperature data and are capable of using moonlight to acquire visible-light images at night since 1965. As one of the primary sensors, the OLS acquired year-round stable NTL imagery with an original spatial resolution of 30 arc-second. These stable NTL imageries were extensively used to monitor time-serial changes in visible-light emissions of urban areas, to estimate the degrees of social and economic developments of communities, to study and monitor volcanic eruptions, etc. [13–17]. However, because of the limited range of the sensor sensitivity of the OLS, the occurrence of pixel saturation in imageries from urban cores makes it difficult to identify and differentiate various types and degrees of socio-economic activities, states, and changes taking place within different parts of cities [18–20]. Thus, a requirement exists for a model that could readily and comprehensively resolve the various spatial features of city areas. Taking 2013 as the time node, we utilized average visible, stable lights, and cloud free coverage F18 2013 NTL composite data as correction object. Downloaded from the NOAA National Geophysical Data Center, the data was re-projected to Albers Equal-Area Conical projection and simultaneously resampled at 1-km spatial resolution using the nearest-neighbor resampling method.

The Suomi National Polar-orbiting Partnership (NPP) Visible Infrared Imaging Radiometer Suite (VIIRS) set up by The Earth Observations Group (EOG) is a scanning imaging radiometer that could collect images of land, clouds, ice, and oceans in the visible and infrared radiation bands. Among the large collection of image datasets, a type of NTL data, designated as Version 1 Nighttime VIIRS Day/Night Band Composites (NPP/VIIRS DNB), can provide supplementary information that can be compared with the saturated DMSP/OLS NTL data. The NPP/VIIRS DNB imageries have improved temporal (monthly vs. yearly availability) and spatial (15 arc-second vs. 30 arc-second, 400 m at sub-satellite points) resolutions compared with those of DMSP/OLS NTL. The NPP/VIIRS DNB Cloud Free Composites 2013 monthly data were employed for validating the accuracy of LST-and-EVI-regulated-NTL-city index (LERNCI). An annual NPP/VIIRS DNB dataset was derived from averaged monthly values from January to December. NPP/VIIRS DNB imageries have not excluded temporal lights from other sources such as fires, volcanic emissions, auroras, etc, and abnormal negative values have been detected in these images. Hence, the quality of the NPP/VIIRS DNB datasets for the selected sample area(s) was checked before these imageries were incorporated into this study [21].

## 2.2. Auxiliary Data

The Earth Observation System (EOS), initiated by the National Aeronautics and Space Administration (NASA), is an integrated system consisting mainly of a series of low-earth-orbit satellites programmed to continuously observe and record natural earth processes. The Moderate-resolution Imaging Spectroradiometer (MODIS) is a primary sensor aboard the Terra and Aqua series of satellites. MODIS sensors can take measurements in 36 discrete spectral bands with spectral band widths ranging from 0.4  $\mu\text{m}$  to 14.4  $\mu\text{m}$ . MODIS has spatial resolutions of 250 m, 500 m, and 1000 m. MODIS can obtain global observation data on a daily or two-day basis. MODIS provided continuous spatial-temporal LST and EVI datasets for this study.

MOD11A2 eight days synthesized 1-km-resolution LST Day-and-Night data and 1-km-resolution MOD13A3 monthly EVI and Normalized Difference Vegetation Index (NDVI) band data were acquired from the Terra platform. To maintain the stability of the data, we calculated the 2013 annual weighted mean instead of emphasizing extreme values. In addition, as light diffraction made the city regional water body also get NTL value, which could be treated as background noise, MOD44W 250-m land-water mask image was used to remove water body pixels as their specific albedo in near infrared and red band lead to negative EVI values.

We obtained the Landsat 8 Operational Land Imager (OLI) data from NASA and the United States Geological Survey (USGS), and the Landsat 8 OLI data with 30-m spatial resolution and 11 bands was used here as a reference to validate the capability of the EVI and LST regulated city index in expressing internal structure of cities such as the central business districts, airports, and urban green spaces.

Considering that the saturated DMSP/OLS region is highly related to human productive activities as well as to population aggregation, a kind of population density data set called WorldPop was introduced here to carry out correlation analyses between different index adjusted city indices and population density. WorldPop is an open-access archive of global-scale spatial demographic distributions taken at five-year intervals beginning in 2010. There are two main mapping methods in WorldPop: random forest regression tree and land-cover based. The former has significantly improved output accuracy more than the latter [22,23]. In addition, WorldPop population estimates at a spatial resolution of approximately 100 m.

### 3. Methods

#### 3.1. Vegetation Adjusted NTL Urban Index

Pozzi and Small [24] showed that there was a significant negative correlation between vegetation density and urban centrality. Within a certain range, vegetation abundance declines toward the center of the impervious surface area (ISA) of a city. Based on this observation, Zhang [25] proposed the VANUI. The VANUI used the NDVI to increase the internal differences in the saturation region (Equation (1)).

$$\text{VANUI} = (1.0 - \text{NDVI}) \times \text{NTL} \quad (1)$$

However, this method only considered a physical geographic indicator, namely the spatial distribution difference of vegetation in the process of construction, ignoring the impact of artificial factors in the evolution of the internal structures of cities. The method performed satisfactorily in reducing saturation on images of highly stable urban areas in developed countries, but was unable to provide sufficient contrast among pixel values from saturated portions of images of cities (such as Beijing and Shanghai) that have recently been undergoing rapid changes in patterns of vegetation cover. In addition, other studies have shown that when the NDVI is higher than 0.7, the area could be treated as a zone with a dense vegetation cover [26–28]. It became evident that a region with NDVI higher than 0.7 could hardly be classifiable as an urban district or even a peri-urban area. As a result, the value of 1.0 in Equation (1) cannot be assumed and the corresponding VANUI values were disproportionally larger than the actual conditions on the ground as an NDVI value of 1.0 corresponds to super-vegetation areas, which are normally located far from any urban area.

#### 3.2. LST- and EVI-Regulated NTL City Index

Taking into account the advantages of EVI in decreasing interference arising from the ground and atmospheric particles, EVI has some advantages compared to NDVI. EVI is less susceptible to saturation by reflected green-colored radiation than NDVI.

As one of the main products of human civilization, an urbanized area has its own distinct properties compared with those of a natural area. There are a large number of artificial structures (such as concrete and asphalt pavements and various building walls), but there are few patches of vegetation in the urban core; thus altering the underlying surface thermodynamic properties. Artificial structures have smaller specific heat capacities compared with surfaces overlaid by natural structures such as green spaces, soils, water bodies, etc. Consequently, urban-core LSTs are usually significantly higher than those of the natural underlying surfaces given the same solar-radiation conditions. Consequently, LST is commonly used to study the urban-heat-island effect. Experimental results indicate that properties of impervious surfaces have a close relation with both LST and vegetation cover [29–31]. By extension, results of correlation analyses reveal that city center degrees tend to be positively correlated with LST and negatively correlated with EVI [32]. Thus, we propose an index incorporating both EVI and LST to regulate images of NTL- saturated urban areas.

LERNCI is defined as:

$$\text{LERNCI} = \text{NOR}\left(\left(\frac{\text{LST}}{\text{LSTAVG}_s} + \frac{\text{EVI}}{\text{EVI}_{\text{AVG}_s}}\right) \times \text{NTL}\right) \quad (2)$$

where LST, EVI, NTL stand for the corresponding values of pixels to be corrected, respectively. LSTAVG<sub>s</sub>, EVI<sub>AVG<sub>s</sub></sub> are average values of all the saturated NTL pixels in the specific regions that represent the mean averages of LSTs and EVIs of the saturated pixels. Parameters and final results are normalized to a range of [0, 1.0] in order to conveniently carry out consistency comparisons.

The LERNCI is based on the assumption that the NTL images are positively related to LSTs and negatively related to EVIs [8–11]. Here, LERNCI is proposed based on the common observation that, as a result of high population densities, levels of human activities, and numbers of artificial structures, the closer to the city center an area is, the higher the LST. Furthermore, it can be readily observed that the amount of vegetation cover decreases as both the impervious surface construction and urban population growth increase. We expect that LERNCI could act on the saturated area of the city center and effectively distinguish the saturated and peri-saturated regions of urban spatial patterns and provide details of changed regions across the globe.

### 3.3. Validation Methodology

The results are validated and verified in four stages.

- (1) The Landsat 8 OLI image data with a 30 m spatial resolution was compared separately with both high and low LERNCI regional values in NTL-saturated city areas to validate the matching status in different urban function areas.
- (2) We selected typical NTL-saturated urban regions from countries in Asia, North America, Africa and Europe and obtained the LERNCI and VANUI of each sample region. By doing so, comparisons could possibly validate the saturation-lowering effect of LERNCI over regions at different latitudes and climatic zones. Additionally, LERNCI could also be used to show the increasing regional trends in the saturated domain of NTL-saturated urban cores, both in developing and developed countries. In recent decades, metropolises in developing countries have experienced significant changes in vegetation-cover patterns due to rapid economic development. At the same time, large cities in developed countries have already gained long-term stability of vegetation-cover patterns at NTL-saturated urban regions.
- (3) The linear regression equations were established between LERNCI, VANUI and NPP/VIIRS DNB data. Then, the correlation coefficients of LERNCI, VANUI and DNB data were calculated and compared to validate the correspondence among LERNCI, VANUI, and NPP/VIIRS DNB datasets.
- (4) Since nighttime luminance could mirror the spatial distribution of human productive activities and aggregation, parameter-adjusted, non-saturated nighttime pixel values could also be suggested to have a corresponding correlation with population density. A series of sample pixels were randomly selected to evaluate the correspondence among LERNCI, VANUI, and demographic distribution data from WorldPop which is an open-access archive of global-scale spatial demographic distributions.

## 4. Results and Analysis

### 4.1. LERNCI for Delineating the Internal Structures of Cities

LERNCI is proposed to be applicable for distinguishing light-intensity differences in urban-core areas and, consequently, for improving image-element resolution in NTL-saturated regions to allow the identification of urban-core structures. Beijing and New York City were selected to validate the effectiveness of LERNCI. As the capital of China, Beijing is one of the biggest cities in the world that has gone through rapid growth and significant changes in urban patterns during the previous three decades. New York City is a typical highly developed city with a relatively stable spatial pattern that



has lasted for decades. These two selected cities could, to some extent, represent the metropolitan characteristics and scales found in developing and developed countries, respectively.

Figures 1 and 2 present both the original NTL images and the results of LERNCI obtained for both Beijing and New York City. Three sample areas in each city were then selected and their outlines were drawn to differentiate their lineaments. It needs to be emphasized that the lineaments were created based on the results of LERNCI rather than using the Landsat 8 images as reference. Also, in order to select images with as little cloud coverage (CC) as possible during vegetation-growing season, we chose Landsat 8 images of Beijing and New York on 12 May 2013 and 15 September 2013 separately, and employed false-color composite images by combining images obtained from the NIR (near infrared), red, and green wavelength bands. In Figure 1a, we chose three areas in Beijing where the LERNCI of pixels were remarkably higher or lower than those of the surrounding regions, but the pixel values in these areas in the original NTL images were all high (saturated) and it was difficult to discriminate between them. These areas were separately labeled as A, B, C. Then, ranges were compared with those from corresponding Landsat 8 images and it was discovered that there existed comparatively high consistencies in the scaled-out ranges for A, B, C, the Central Business District (CBD) around the Forbidden City, Beijing International Airport, and the Beijing Olympic Forest Park. Similarly, three areas that stand out from the surrounding regions were selected in New York City and labeled as A, B, and C. The matching results in Landsat 8 imagery showed a relatively close correlation between the lined-out dissimilar LERNCI ranges and the ranges obtained at the Newark Airport, Brooklyn Central blocks, and at an area consisting of the High Land Park, the St. John Cemetery and the Lutheran All Faiths Cemetery, respectively. Figures 1 and 2 indicate that the polygon regions marked out by referring to LERNCI did not precisely correspond with the shapes of the target features. This situation resulted from the common existence of mixed pixels in the border regions of the target features, which resulted in LERNCI variability for these boundary pixels.

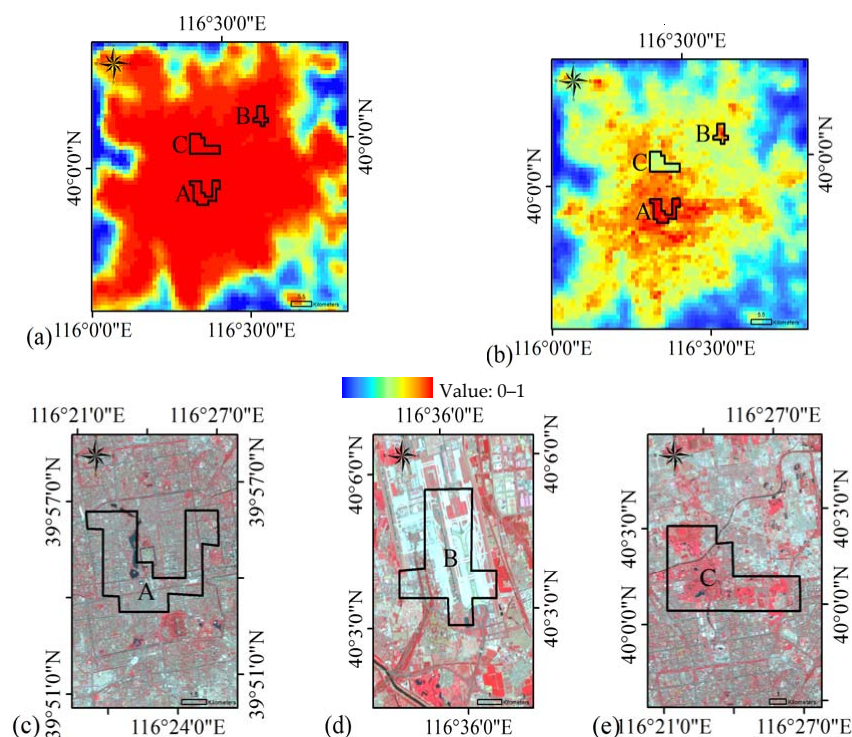


**Figure 1.** Raw Night Time Lights (NTL) image (a) and Land Surface Temperature (LST)-and-Enhanced Vegetation Index (EVI)-regulated-NTL-city index (LERNCI) result (b) of Beijing and corresponding Landsat 8 images with black boundary polygons. (c): A, Central business district (CBD) around the Forbidden City; (d): B, Beijing International Airport; (e): C, Beijing Olympic Forest Park.

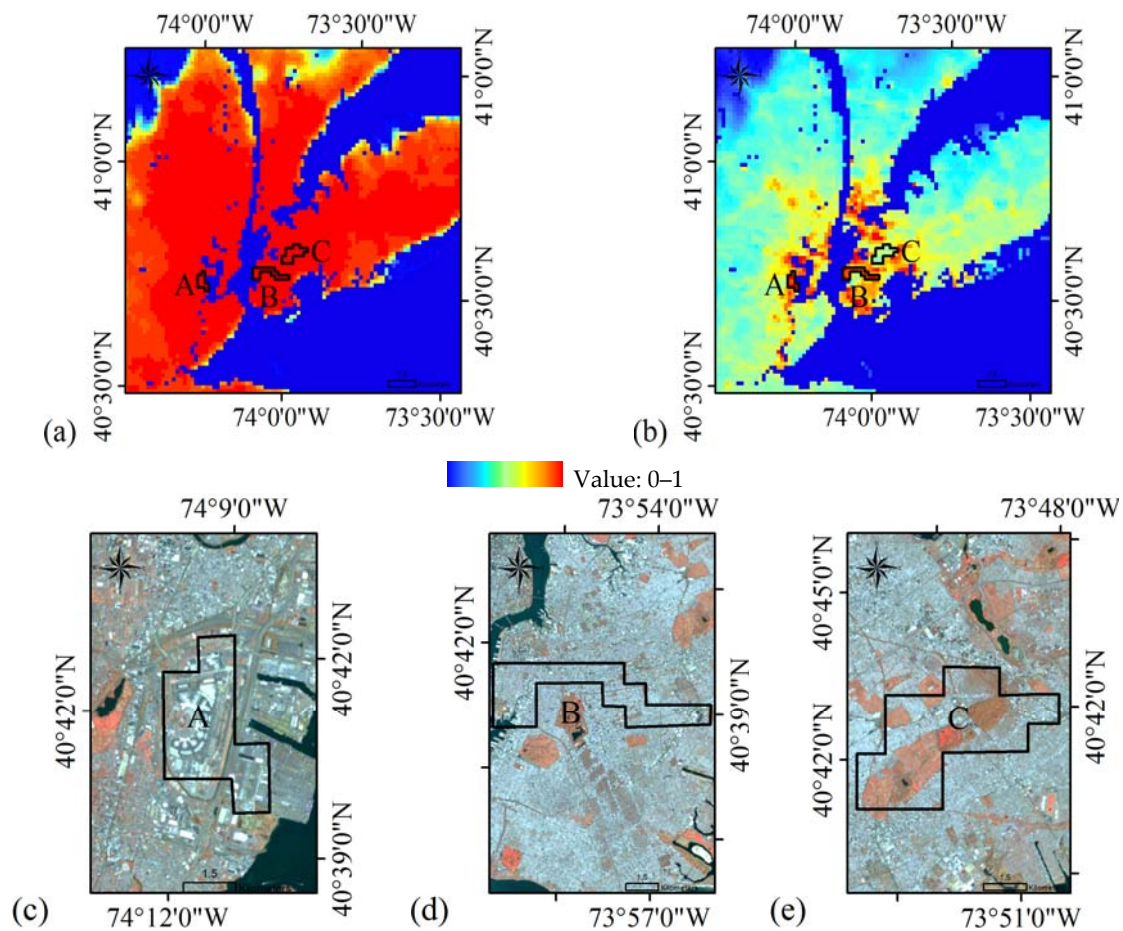


**Figure 2.** Raw NTL image (a) and LERNCI result (b) of New York and corresponding Landsat 8 with black boundary polygons. (c): A, Newark airport; (d): B, Brooklyn central blocks; (e): C, combination of High Land Park, the St John Cemetery and the Lutheran All Faiths Cemetery.

#### 4.2. Visual Comparison of NTL, VANUI and LERNCI

Because of the common occurrence of large-area saturation in conurbation core areas, it becomes difficult to distinguish the inner spatial structures and functional subzones of a certain city. Thus, adjustment by correlated remote sensing data is an essential prerequisite for decreasing the sizes of saturated regions as well as increasing spatial differentiation. Here we chose ten large cities across the world to compare and analyze their different performances in expressing inter-urban variations (Figures 3 and 4). Five metropolises selected from developing countries include Beijing, Seoul, New Delhi, Mexico City, and Lagos, respectively belonging to China, South Korea, India, Mexico and Nigeria. Correspondingly, the other five examples which stand for typical stable post-industrial cities are New York City, NY, USA; Tokyo, Japan; London, UK; Moscow, Russia; and Los Angeles, CA, USA.

Apparently, raw images could barely provide any information about interior details and land-cover changes for all of the samples. Both LERNCI and VANUI can, to some degree, reflect spatial varieties, especially for green/vegetation-rich areas, business districts and built environments within a city. Nevertheless, it is commonly suggested that, although there could have been large coverage of built-up urban areas and CBDs, these regions can be divided into different levels that indicate corresponding degrees of centrality for a particular area; or instance, town center, peri-urban core, auxiliary city center, and conurbation core areas. Overall, VANUI can make a clear distinction between built-up environments and green zones, and could efficiently show impervious-surface extents within inner urban areas in samples from highly developed countries such as New York City, London, and

Moscow. However, VANUI performs less satisfactorily when recognizing the hierarchies of peri-urban and urban-center degrees in all the other samples, especially in the mega cities of developing countries as there are many areas of similar high values represented in the city regions by orange and red colors. In contrast, LERNCI could legibly and effectively use remarkably different values to elucidate the variability of constructed areas such as those in Beijing, New Delhi, Mexico City, and Tokyo.

As a general rule, urbanization results in biotic homogenization [33] and the whole area of a city becomes confined within a single climate zone. However, even though EVIs could be identical within a certain region inside an urban area, LST may not respond equally since artificial elements such as local population densities, construction densities, percentages of impervious surfaces, amounts of electricity consumption, etc. could influence zone temperatures. These elements could also contribute to the urban-heat-island effect, which means the area could get warmer because of the higher concentration of artificial elements and in spite of the existence of a constant vegetation index, and this indicator derived from the ISA always is highly correlatable with the degree of closeness to the regional center. Thus, the change of LST would deeply influence LERNCI value while VANUI does not take this indicator into consideration [34–37].

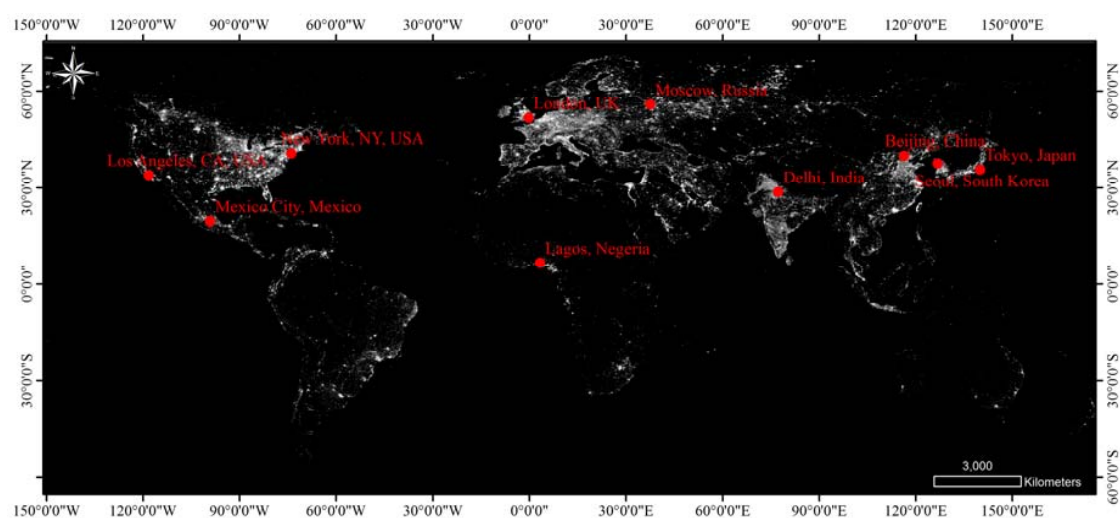


**Figure 3.** Operational Linescan System of the US Defense Meteorological Satellite Program (DMSP/OLS) NTL image of the world in 2013 and samples selected from NTL saturated areas.

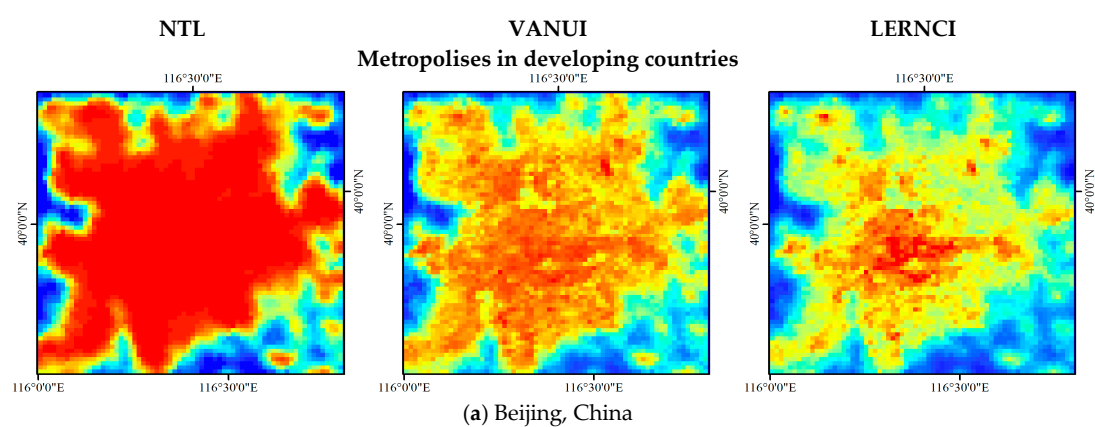


**Figure 4.** Cont.



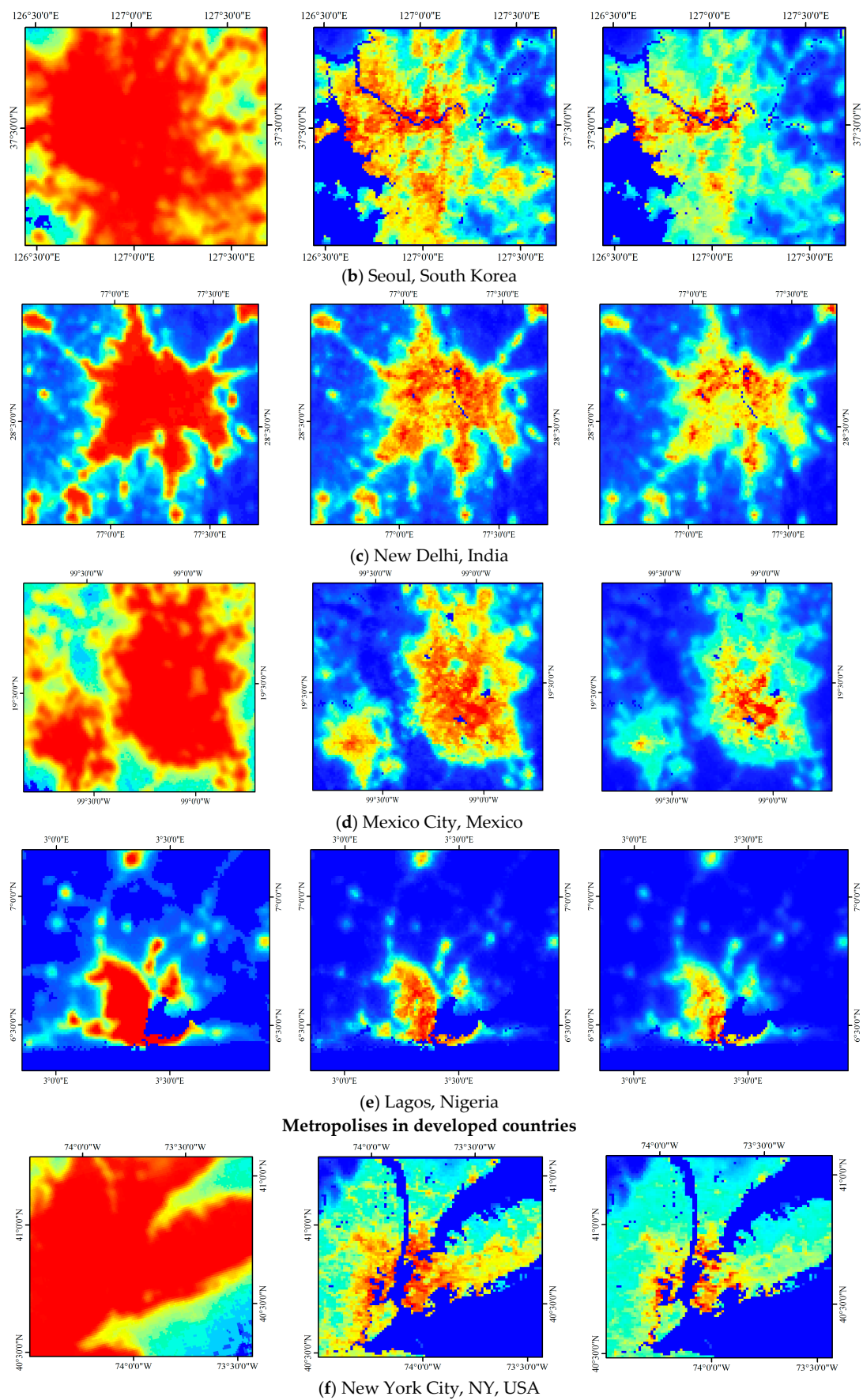
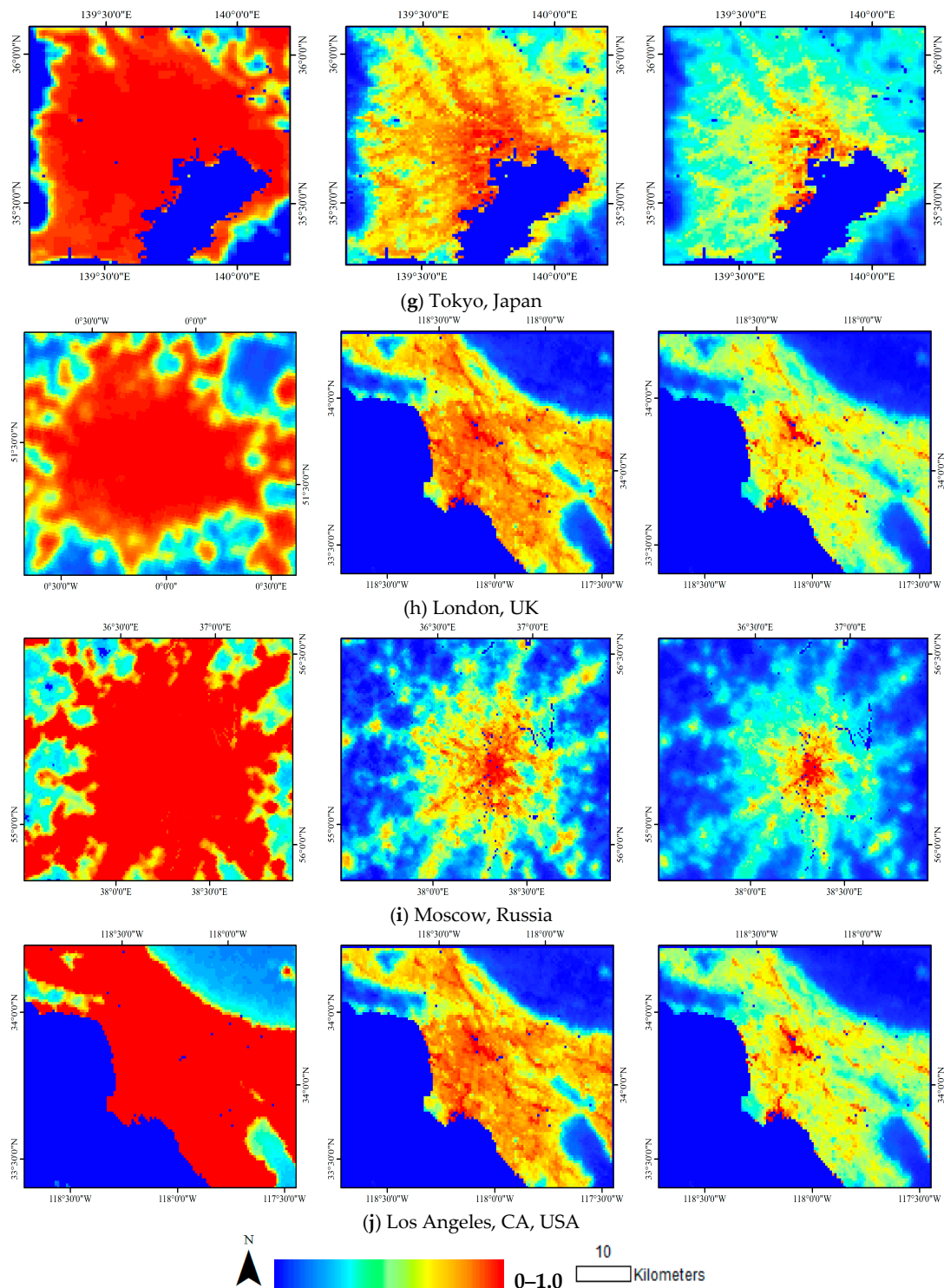


Figure 4. Cont.



**Figure 4.** Comparison among original NTL images, Vegetation Adjusted NTL Urban Index (VANUI), and LERNCI-validated results in metropolises from both developing and developed countries: (a) Beijing, China; (b) Seoul, South Korea; (c) New Delhi, India; (d) Mexico City, Mexico; (e) Lagos, Nigeria; (f) New York City, NY, USA; (g) Tokyo, Japan; (h) London, UK; (i) Moscow, Russia; (j) Los Angeles, CA, USA.

#### 4.3. Correlation Analysis with NPP/VIIRS DNB Dataset

NASA set up the NPP in 2011 to monitor both the environment and the atmosphere of the earth and continue global environmental observations. One data product, the NPP/VIIRS DNB, solves the problem of NTL saturation and further enhances spatial resolution to 400 m along the sub-satellite point. Considering that version 1 NPP/VIIRS DNB data has not filtered out random temporal light noise and this paper is mainly devoted to studying the quantification of a regional city index, NPP/VIIRS DNB is treated as an evaluating indicator here.

We selected Beijing and Lagos as the sample of developing countries and Tokyo as the sample of developed countries individually and Delhi, Seoul as the developing city samples of torrid zone. Then 1000 random points were produced from corresponding areas to validate their correlation with NPP/VIIRS DNB data. Beijing has a typical continental-temperate-monsoon climate with four distinctive seasons. Its annual average temperature is around 10 to 12 degrees centigrade and its mean annual precipitation is about 600 mm. Tokyo, accompanied by distinct and moderate seasons, belongs to the oceanic-temperate-monsoon climate zone. There is an annual average precipitation of about 1800 mm in Tokyo, which is three times that of Beijing. Lagos belongs to the tropical-savanna climate and has an annual average temperature of 26 to 27 degrees centigrade. Its rainy season lasts for 7 months from April onwards, and the dry season lasts for 5 months, from November to March. New Delhi has a tropical-monsoon climate with warm, dry winters (mean temperature is about 14 degrees centigrade) and hot, rainy summers (mean temperature is about 38 degrees centigrade). Although Seoul also belongs to the continental-monsoon climate with an annual mean temperature of 11.8 degrees centigrade, its climate is more oceanic as South Korea is surrounded by seas on three sides and is characterized by a narrower annual temperature range and greater amounts of precipitation than that in Beijing.

Figure 5 demonstrates a scatterplot as well as a regression line of LERNCI and VANUI against NPP/VIIRS DNB. Randomly generated points (1000 in number) were located within each city core area domain of Figure 4. NPP/VIIRS DNB images have been re-sampled to 1-km spatial resolution to maintain consistent spatial resolution. For the sake of sufficient representative power for the total data set and the avoidance of repetition, the minimum distance between any two random points is set to 1 km. The values of VANUI can obviously be larger than those of LERNCI, in general. This indicates again that the value of 1.0 in Equation (1) was not reasonable; therefore, the VANUI value was obviously larger than the actual value as an NDVI value of 1.0 corresponds to super-vegetation areas that would be located far from any urban or peri-urban area. Moreover, it seemed that the two groups of scatterplots (blue and red) had similar shapes. Nevertheless, the  $R^2$  between the VANUI and NPP/VIIRS DNB was 0.76 in Beijing, 0.77 in Lagos, 0.84 in Tokyo, 0.89 in New Delhi, and 0.83 in Seoul, less than the  $R^2$  between LERNCI and NPP/VIIRS DNB.

The WorldPop project was initiated in 2013 and is composed of AfriPop, AsiaPop, and AmeriPop. This project provides open-access population distribution datasets using transparent mapping approaches to measure and predict population variations. While nighttime luminance could not directly indicate local population densities, previous researches suggested that it has a close relation to the spatial distribution of human productive activities and aggregation in urban regions, which means parameter-adjusted, non-saturated NTLs could also have a correlative association with population density [38–42]. Beijing, Lagos, Tokyo, New Delhi, and Seoul were selected for comparison of LERNCI to VANUI in expressing spatial demographic distributions in city areas. Since the WorldPop datasets include data starting from 2010 and have a temporal resolution of 5 years, the 2015 demographic-distribution data collection was chosen to validate the correlation. It is necessary to note that the mapping approach for Beijing (Figure 6a), Lagos (Figure 6b), and Seoul (Figure 6e) was random-forest based; and that for Tokyo (Figure 6c) and New Delhi (Figure 6d) it was land-cover based. WorldPop data was re-sampled to 1-km resolution before being randomly selected. Then we regressed LERNCI on Population Density and VANUI on Population Density individually. Equally, it seemed that the two groups of scatterplots (blue and red) had similar shapes; and values of VANUI

(blue) are higher than those of LERNCI (red). Still, coefficient of determination results stated clearly that Population Density and LERNCI always had a relatively higher  $R^2$  of 0.72 in Beijing, 0.68 in Lagos, 0.66 in Tokyo, 0.39 in New Delhi, and 0.47 in Seoul. In contrast, the  $R^2$  for Population Density and VANUI were merely 0.58 in Beijing, 0.67 in Lagos, 0.65 in Tokyo, 0.33 in New Delhi, and 0.42 in Seoul.

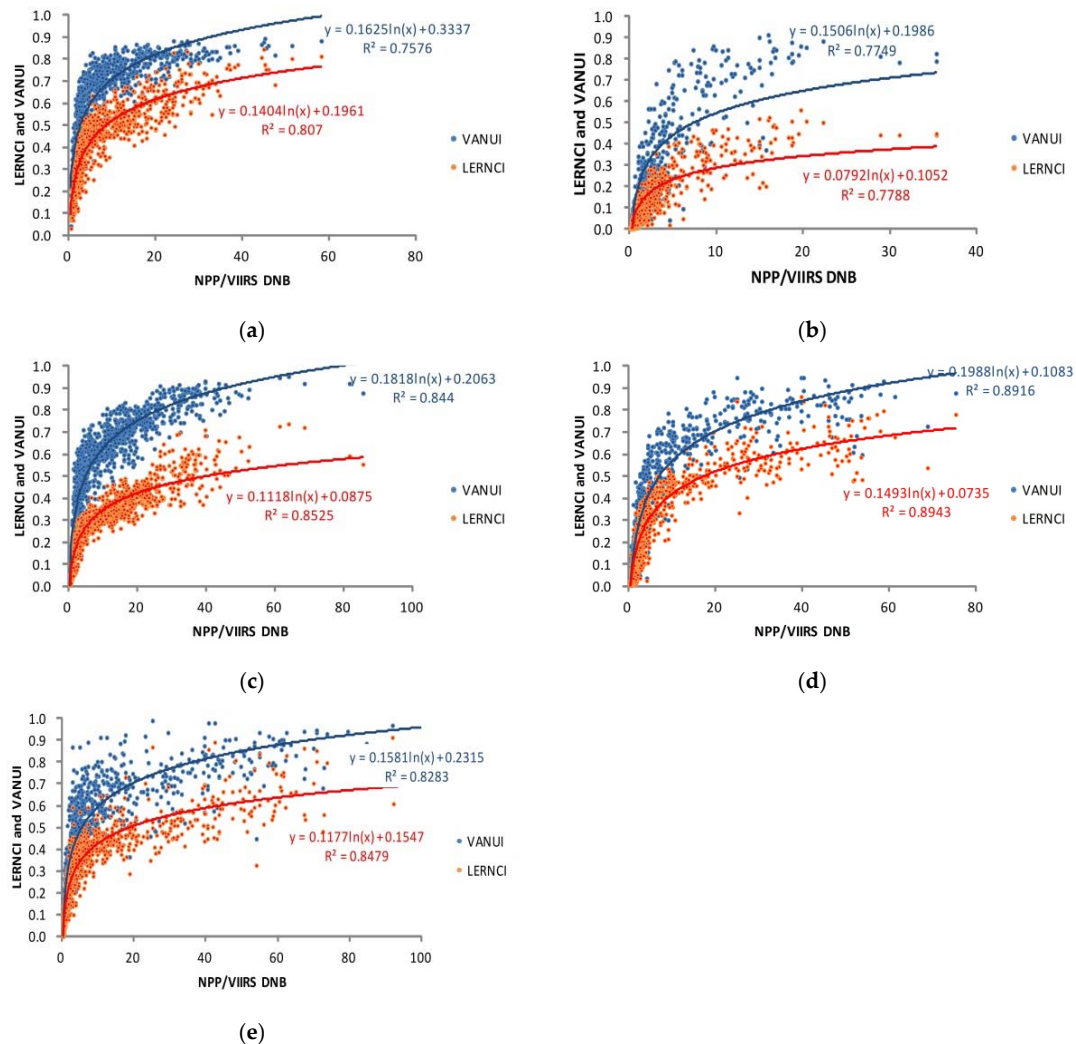


**Figure 5.** Scatterplot of LERNCI and VANUI against Version 1 Nighttime Visible Infrared Imaging Radiometer Suite Day/Night Band Composite (NPP/VIIRS DNB) of (a) Beijing (b) Lagos (c) Tokyo (d) New Delhi (e) Seoul. The solid lines correspond to regression line. 4.4 Comparison between LERNCI and VANUI in characterizing population density.

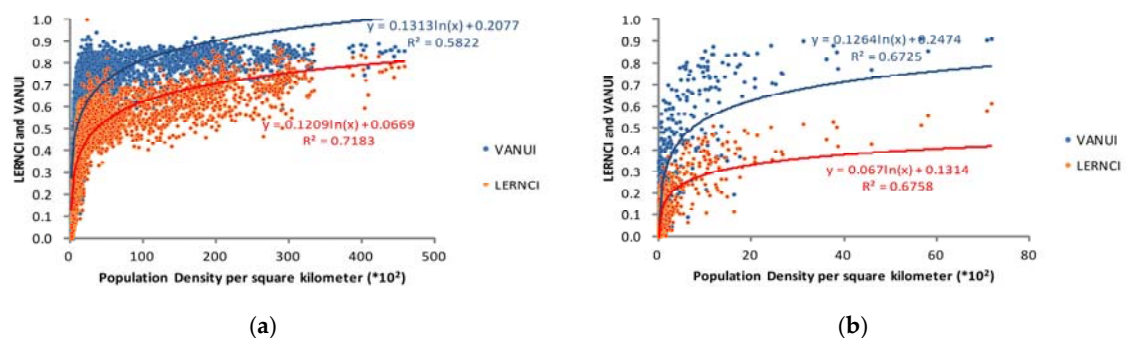


**Figure 6.** Cont.



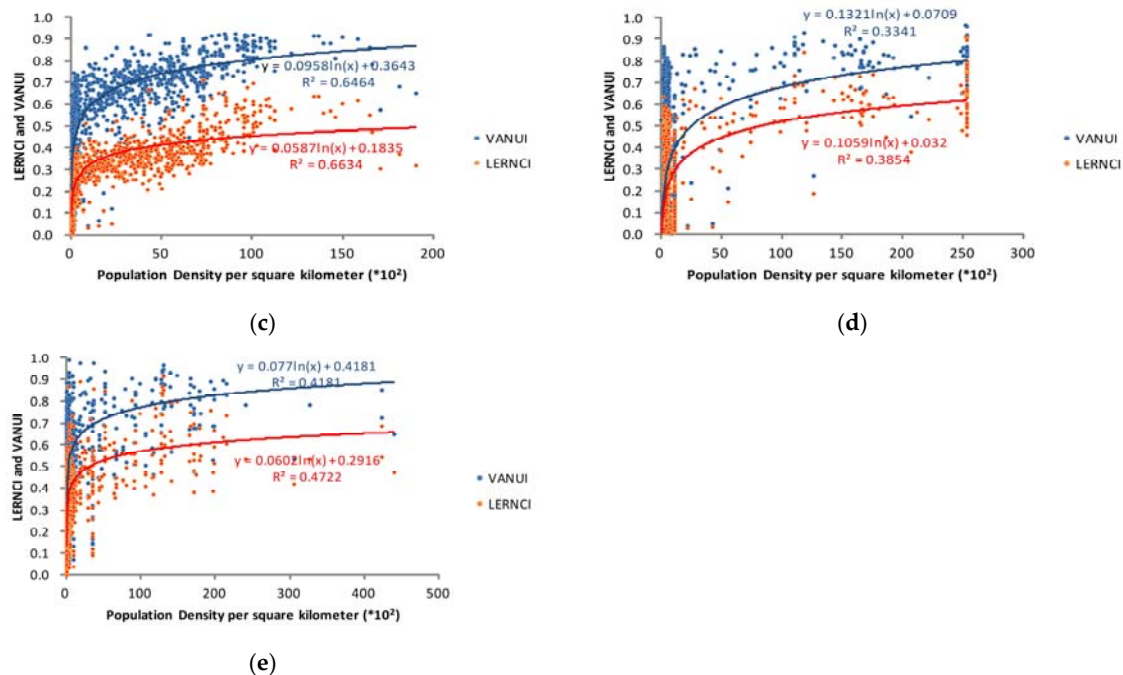


**Figure 6.** Scatterplots of LERNCI and VANUI against Population Density of (a) Beijing (b) Lagos (c) Tokyo (d) New Delhi (e) Seoul. The solid lines correspond to the logarithmic regression line.

## 5. Discussion

In this study, we proposed an index to regulate saturated DMSP/OLS NTL data using vegetation cover and urban temperatures via MODIS EVI and LST datasets. Ten cities were selected around the world from NTL-saturated regions (Figure 3) to validate the performance of LERNCI in delineating the inner structures of urban areas. LERNCI could subsequently convey the distribution patterns of urban impervious surface areas and, to some extent, characterize local population aggregation trends. The LERNCI addresses the NTL-saturation problem in urban-core areas with a high degree of accuracy and can become a valuable tool for urban internal differentiation.

Regulated by EVI and LST, LERNCI can effectively express spatial differences that are correlatable to vegetation structure and LST in NTL-saturated urban-core areas. Previous studies showed that human activities become more concentrated as the distance gets closer to the city center, which means higher demographic densities, higher ratios of impervious surface areas, lower ratios of vegetation cover and correspondingly more pronounced urban-heat-island effects in urban core areas [43–45]. In addition, in consideration of regional specific vegetational zonality structure and underlying surface features, we proposed LERNCI (Equation (2)) with combination of EVI and LST to regulate NTL-saturated urban area images. As a result, we could easily identify central CBDs, airports, green zones, and cemeteries from high and low LERNCI values inside NTL peri-saturated and saturated city areas. In addition, when compared to VANUI [25], which is only adjusted by NDVI, LERNCI improves the capability in appropriately outlining urban inner structures with significant applications, especially in developing countries with unstable regional vegetation patterns. Moreover, LERNCI shows a more prominent relevance to both NPP/VIIRS DNB data sets and Population Density data collection from WorldPop.  $R^2$  between LERNCI and NPP/VIIRS DNB was 0.81 in Beijing, 0.78 in Lagos, 0.85 in Tokyo, 0.89 in New Delhi, and 0.85 in Seoul, which is superior than the  $R^2$  between VANUI and NPP/VIIRS DNB. Also, there was a closer logarithmic regression relationship between LERNCI and population density. LERNCI had a relatively higher  $R^2$  of 0.72 in Beijing, 0.68 in Lagos, 0.66 in Tokyo, 0.38 in New Delhi, and 0.47 in Seoul compared with the  $R^2$  for Population Density and VANUI, which are 0.58 in Beijing, 0.67 in Lagos, 0.65 in Tokyo, 0.33 in New Delhi, and 0.42 in Seoul. Thus,

it could also perform as a helpful reference data for acquiring comprehensive diversified urban-form images. However, there are still some limitations in LERNCI because it is based on vegetation cover and the urban-heat-island effect. It may, for example, not perform well in cities located in arid or semi-arid climates with poor vegetation cover. Also, it can be difficult for LERNCI to work effectively in cities with comparatively uniform population distributions and gradually changing urban core LSTs. Moreover, there exist three special cases regarding NTL images. Firstly, fringe suburbs such as those in Karamay, Tarim Basin oil-and-gas fields in northwest China and the oil-and-gas fields in the Congo, Equatorial Guinea, Gabon that often have fewer populated urban features but higher NTL intensities that originate from oil-and-gas production facilities. Therefore, NTL pixel values could barely indicate urban development levels under such circumstances. Also, compared to less-developed cities with high luminance, deserted ghost towns, such as Erdos in the Inner Mongolia Autonomous Region of China, have low-luminance massive built-up areas that are mostly uninhabited. As a result of the decline of supporting industries, these ghost towns seem obscure at night. Finally, developed countries do not constitute a homogeneous group with constantly high NTL-saturated signatures. For example, Nordic countries such as Denmark, Finland, Sweden, and Norway that have extensive urban infrastructures, frigid weathers, and sparse populations all have relatively low levels of NTL emissions.

This study has taken a step in the direction of describing the regional variation of saturated DMSP/OLS NTL data. Given the connection between LERNCI and urban impervious surface areas, population densities, rates of energy consumption, and ratios of urban greening, LERNCI can prove useful for urban-pattern planning and for easing the central functions of metropolises.

## 6. Conclusions

Based on NDVI being negatively correlated with urban centrality, Zhang came up with a formula (Equation (1)) called VANUI, which performs satisfactorily for decreasing saturation and increasing inter-urban variation [25]. However, VANUI takes NDVI as the only reference to adjust for NTL saturation, which ignores regional temperature increases that result from the urban-heat-island effect, in turn brought about by impervious surface areas and high density buildings in favor of the inherent predominant vegetation patterns. Furthermore, the value of 1.0 in Equation (1) presupposes a maximum value of NDVI appropriate only for dense forests, which are likely located far away from any ordinary urban or peri-urban area. Hence, it seems to have a poor performance in mapping urban structures in developing countries with unstable vegetation distributions.

To overcome the shortcomings of VANUI and to address the DMSP/OLS NTL-saturation phenomenon, we proposed a LERNCI on considering that the degree of proximity towards the city center can have a positive correlation with temperature and negative correlation with vegetation coverage. Compared with NDVI, EVI performs better against soil-noise interference and against mid-visible-spectrum saturation. The validation results showed that we could rapidly identify the positions and profiles of CBDs and urban green spaces by using LERNCI. LERNCI-adjusted NTL images also gained superior discrimination of inner-city forms especially in samples from developing countries than VANUI-corrected images. Further, the validation results reveal a closer goodness-of-fit relationship with both NPP/VIRS DNB data and WorldPop population density data for LERNCI-enhanced images than for VANUI-enhanced images.

Though LERNCI can explicitly resolve variations of inner urban spaces, more indices such as those for carbon dioxide emissions, industrial spatial-distribution structures, etc. are required to acquire a more accurate city index in the future. Also, resolutions exceeding 1km could provide finer details about urban forms. In addition, as regulated by EVI and LST, LERNCI may not perform effectively in cities with sparse vegetation cover or in areas characterized with gradually increasing urban-core LSTs. Thus, further research would be required for designing multi-parameter-regulated NTL city indices that have finer urban center luminance-variation resolutions.

**Acknowledgments:** The authors wish to thank the China Knowledge Center for Engineering Sciences and Technology (No. CKCEST-2015-1-4), the National Special Program on Basic Science and Technology Research

of China (No. 2013FY110900) and the Data Sharing Infrastructure of Earth System Science for financial support. We are indebted to the National Aeronautics and Space Administration and the United States Geological Survey for providing MODIS and Landsat 8 data, National Oceanic and Atmosphere Administration for providing and NPP/VIIRS DNB data and WorldPop for providing 2015 population density data.

**Author Contributions:** Yangxiaoyue Liu conceived the research then drafted the manuscript. Yaping Yang, Ling Yao and Wenlong Jing designed the research and reviewed the manuscript. Xiafang Yue and Xiaodan Zhao collected all the data employed in this paper and explained the results. All the authors contributed to editing and reviewing the manuscript.

**Conflicts of Interest:** The authors declare no conflict of interest.

## References

- Seto, K.C.; Fragkias, M.; Güneralp, B.; Reilly, M.K. A meta-analysis of global urban land expansion. *PLoS ONE* **2011**, *6*, e23777. [[CrossRef](#)] [[PubMed](#)]
- Seto, K.C.; Kaufmann, R.K.; Woodcock, C.E. Landsat reveals China's farmland reserves, but they're vanishing fast. *Nature* **2000**, *406*, 121. [[CrossRef](#)] [[PubMed](#)]
- Jing, W.; Yang, Y.; Yue, X.; Zhao, X. Mapping Urban Areas with Integration of DMSP/OLS Nighttime Light and MODIS Data Using Machine Learning Techniques. *Remote Sens.* **2015**, *7*, 12419–12439. [[CrossRef](#)]
- Zhang, Q.; Seto, K.C. Mapping urbanization dynamics at regional and global scales using multi-temporal DMSP/OLS nighttime light data. *Remote Sens. Environ.* **2011**, *115*, 2320–2329. [[CrossRef](#)]
- Letu, H.; Hara, M.; Yagi, H.; Naoki, K.; Tana, G.; Nishio, F.; Shuhei, O. Estimating energy consumption from night-time DMSP/OLS imagery after correcting for saturation effects. *Int. J. Remote Sens.* **2010**, *31*, 4443–4458. [[CrossRef](#)]
- Letu, H.; Hara, M.; Tana, G.; Nishio, F. A saturated light correction method for DMSP/OLS nighttime satellite imagery. *IEEE Trans. Geosci. Remote Sens.* **2012**, *50*, 389–396. [[CrossRef](#)]
- Ziskin, D.; Baugh, K.; Hsu, F.-C.; Elvidge, C.D. Methods used for the 2006 radiance lights. *Proc. Asia-Pac. Adv. Netw.* **2010**. [[CrossRef](#)]
- Zhuo, L.; Zhang, X.; Zheng, J.; Tao, H.; Guo, Y. An EVI-based method to reduce saturation of DMSP/OLS nighttime light data. *Acta Geogr. Sin.* **2015**, *70*, 1339–1350.
- Chen, X.-L.; Zhao, H.-M.; Li, P.-X.; Yin, Z.-Y. Remote sensing image-based analysis of the relationship between urban heat island and land use/cover changes. *Remote Sens. Environ.* **2006**, *104*, 133–146. [[CrossRef](#)]
- Dousset, B.; Gourmelon, F. Satellite multi-sensor data analysis of urban surface temperatures and landcover. *ISPRS J. Photogramm. Remote Sens.* **2003**, *58*, 43–54. [[CrossRef](#)]
- Li, Z.-L.; Tang, B.-H.; Wu, H.; Ren, H.; Yan, G.; Wan, Z.; Trigo, I.F.; Sobrino, J.A. Satellite-derived land surface temperature: Current status and perspectives. *Remote Sens. Environ.* **2013**, *131*, 14–37. [[CrossRef](#)]
- Keller, M.; Kiene, R.; Kirst, G.; Visscher, P. *Biological and Environmental Chemistry of DMSP and Related Sulfonium Compounds*; Springer Science & Business Media: Berlin, Germany, 2012.
- Zhuo, L.; Ichinose, T.; Zheng, J.; Chen, J.; Shi, P.; Li, X. Modelling the population density of China at the pixel level based on DMSP/OLS non-radiance-calibrated night-time light images. *Int. J. Remote Sens.* **2009**, *30*, 1003–1018. [[CrossRef](#)]
- Imhoff, M.L.; Lawrence, W.T.; Stutzer, D.C.; Elvidge, C.D. A technique for using composite DMSP/OLS “city lights” satellite data to map urban area. *Remote Sens. Environ.* **1997**, *61*, 361–370. [[CrossRef](#)]
- Elvidge, C.D.; Safran, J.; Nelson, I.; Tuttle, B.; Hobson, V.R.; Baugh, K.E.; Dietz, J.B.; Erwin, E.H.; Lunetta, R.; Lyon, J. *Area and Positional Accuracy of DMSP Nighttime Lights Data*; CRC Press: Boca Raton, FL, USA, 2004.
- Henderson, M.; Yeh, E.T.; Gong, P.; Elvidge, C.; Baugh, K. Validation of urban boundaries derived from global night-time satellite imagery. *Int. J. Remote Sens.* **2003**, *24*, 595–609. [[CrossRef](#)]
- Small, C.; Pozzi, F.; Elvidge, C.D. Spatial analysis of global urban extent from DMSP-OLS night lights. *Remote Sens. Environ.* **2005**, *96*, 277–291. [[CrossRef](#)]
- Anderson, S.J.; Tuttle, B.T.; Powell, R.L.; Sutton, P.C. Characterizing relationships between population density and nighttime imagery for Denver, Colorado: issues of scale and representation. *Int. J. Remote Sens.* **2010**, *31*, 5733–5746. [[CrossRef](#)]
- Elvidge, C.D.; Erwin, E.H.; Baugh, K.E.; Ziskin, D.; Tuttle, B.T.; Ghosh, T.; Sutton, P.C. Overview of DMSP nighttime lights and future possibilities. In *Proceedings of the 2009 Joint Urban Remote Sensing Event*, Shanghai, China, 20–22 May 2009; pp. 1–5.

20. Elvidge, C.D.; Cinzano, P.; Pettit, D.; Arvesen, J.; Sutton, P.; Small, C.; Nemani, R.; Longcore, T.; Rich, C.; Safran, J. The Nightsat mission concept. *Int. J. Remote Sens.* **2007**, *28*, 2645–2670. [[CrossRef](#)]
21. Shi, K.; Yu, B.; Huang, Y.; Hu, Y.; Yin, B.; Chen, Z.; Chen, L.; Wu, J. Evaluating the ability of NPP-VIIRS nighttime light data to estimate the gross domestic product and the electric power consumption of China at multiple scales: A comparison with DMSP-OLS data. *Remote Sens.* **2014**, *6*, 1705–1724. [[CrossRef](#)]
22. Stevens, F.R.; Gaughan, A.E.; Linard, C.; Tatem, A.J. Disaggregating census data for population mapping using random forests with remotely-sensed and ancillary data. *PLoS ONE* **2015**, *10*, e0107042. [[CrossRef](#)] [[PubMed](#)]
23. Gaughan, A.E.; Stevens, F.R.; Linard, C.; Jia, P.; Tatem, A.J. High resolution population distribution maps for Southeast Asia in 2010 and 2015. *PLoS ONE* **2013**, *8*, e55882. [[CrossRef](#)] [[PubMed](#)]
24. Pozzi, F.; Small, C. Analysis of urban land cover and population density in the United States. *Photogramm. Eng. Remote Sens.* **2005**, *71*, 719–726. [[CrossRef](#)]
25. Zhang, Q.; Schaaf, C.; Seto, K.C. The vegetation adjusted NTL urban index: A new approach to reduce saturation and increase variation in nighttime luminosity. *Remote Sens. Environ.* **2013**, *129*, 32–41. [[CrossRef](#)]
26. Julien, Y.; Sobrino, J.A.; Verhoef, W. Changes in land surface temperatures and NDVI values over Europe between 1982 and 1999. *Remote Sens. Environ.* **2006**, *103*, 43–55. [[CrossRef](#)]
27. Pettorelli, N.; Vik, J.O.; Mysterud, A.; Gaillard, J.M.; Tucker, C.J.; Stenseth, N.C. Using the satellite-derived NDVI to assess ecological responses to environmental change. *Trends Ecol. Evol.* **2005**, *20*, 503–510. [[CrossRef](#)] [[PubMed](#)]
28. Rajasekar, U.; Weng, Q. Urban heat island monitoring and analysis using a non-parametric model: A case study of Indianapolis. *ISPRS J. Photogramm. Remote Sens.* **2009**, *64*, 86–96. [[CrossRef](#)]
29. Yuan, F.; Bauer, M.E. Comparison of impervious surface area and normalized difference vegetation index as indicators of surface urban heat island effects in Landsat imagery. *Remote Sens. Environ.* **2007**, *106*, 375–386. [[CrossRef](#)]
30. Weng, Q.; Lu, D.; Schubring, J. Estimation of land surface temperature–vegetation abundance relationship for urban heat island studies. *Remote Sens. Environ.* **2004**, *89*, 467–483. [[CrossRef](#)]
31. Xiao, R.-B.; Ouyang, Z.-Y.; Zheng, H.; Li, W.-F.; Schienke, E.W.; Wang, X.-K. Spatial pattern of impervious surfaces and their impacts on land surface temperature in Beijing, China. *J. Environ. Sci.* **2007**, *19*, 250–256. [[CrossRef](#)]
32. Zhou, D.; Zhao, S.; Liu, S.; Zhang, L.; Zhu, C. Surface urban heat island in China's 32 major cities: Spatial patterns and drivers. *Remote Sens. Environ.* **2014**, *152*, 51–61. [[CrossRef](#)]
33. McKinney, M.L. Urbanization as a major cause of biotic homogenization. *Biol. Conserv.* **2006**, *127*, 247–260. [[CrossRef](#)]
34. Grimmond, C.; Oke, T.R. Turbulent heat fluxes in urban areas: Observations and a local-scale urban meteorological parameterization scheme (LUMPS). *J. Appl. Meteorol.* **2002**, *41*, 792–810. [[CrossRef](#)]
35. Imhoff, M.L.; Zhang, P.; Wolfe, R.E.; Bounoua, L. Remote sensing of the urban heat island effect across biomes in the continental USA. *Remote Sens. Environ.* **2010**, *114*, 504–513. [[CrossRef](#)]
36. Shepherd, J.M.; Burian, S.J. Detection of urban-induced rainfall anomalies in a major coastal city. *Earth Interact.* **2003**, *7*, 1–17. [[CrossRef](#)]
37. Rosenzweig, C.; Solecki, W.D.; Parshall, L.; Chopping, M.; Pope, G.; Goldberg, R. Characterizing the urban heat island in current and future climates in New Jersey. *Glob. Environ. Chang. Part B Environ. Hazards* **2005**, *6*, 51–62. [[CrossRef](#)]
38. Zhuo, L.; Chen, J.; Shi, P.; Gu, Z.; Fan, Y.; Ichinose, T. Modeling population density of China in 1998 based on DMSP/OLS nighttime light image. *Acta Geogr. Sin.* **2005**, *60*, 266–276.
39. Welch, R. Monitoring urban population and energy utilization patterns from satellite data. *Remote Sens. Environ.* **1980**, *9*, 1–9. [[CrossRef](#)]
40. Cheng, L.; Zhou, Y.; Wang, L.; Wang, S.; Du, C. An estimate of the city population in china using dmSP night-time satellite imagery. In Proceedings of the IEEE International Geoscience and Remote Sensing Symposium (IGARSS 2007), Barcelona, Spain, 23–28 July 2007; pp. 691–694.
41. Sutton, P.C.; Taylor, M.J.; Elvidge, C.D. Using DMSP OLS imagery to characterize urban populations in developed and developing countries. In *Remote Sensing of Urban and Suburban Areas*; Springer: Berlin, Germany, 2010; pp. 329–348.



42. Lo, C. Modeling the population of China using DMSP operational linescan system nighttime data. *Photogramm. Eng. Remote Sens.* **2001**, *67*, 1037–1047.
43. Gallo, K.; McNab, A.; Karl, T.; Brown, J.; Hood, J.; Tarpley, J. The use of NOAA AVHRR data for assessment of the urban heat island effect. *J. Appl. Meteorol.* **1993**, *32*, 899–908. [[CrossRef](#)]
44. Lo, C.P.; Quattrochi, D.A.; Luvall, J.C. Application of high-resolution thermal infrared remote sensing and GIS to assess the urban heat island effect. *Int. J. Remote Sens.* **1997**, *18*, 287–304. [[CrossRef](#)]
45. Gallo, K.P.; Owen, T.W. Satellite-based adjustments for the urban heat island temperature bias. *J. Appl. Meteorol.* **1999**, *38*, 806–813. [[CrossRef](#)]



© 2017 by the authors. Licensee MDPI, Basel, Switzerland. This article is an open access article distributed under the terms and conditions of the Creative Commons Attribution (CC BY) license (<http://creativecommons.org/licenses/by/4.0/>).